Letter Vol. 49, No. 16 / 15 August 2024 / Optics Letters 4713

Optics Letters

Multifrequency nonlinear Schrödinger equation

David Castelló-Lurbe,[1,2,*] Enrique Silvestre,[1,3] and Miguel V. Andrés[1,2]

[1] Institut Universitari de Ciències dels Materials, Universitat de València, Catedrático Agustín Escardino 9, Paterna 46980, Spain
[2] Departament de Física Aplicada i Electromagnetisme, Universitat de València, Dr. Moliner 50, Burjassot 46100, Spain
[3] Departament d'Òptica i Optometria i Ciències de la Visió, Universitat de València, Dr. Moliner 50, Burjassot 46100, Spain
*david.castello-lurbe@uv.es

Received 1 May 2024; revised 27 July 2024; accepted 29 July 2024; posted 30 July 2024; published 14 August 2024

The multifrequency character of nonlinearity dispersion is often dismissed because, in principle, it increases the computational load exceedingly rendering an impractical modeling and, typically, nonlinearities barely depend on frequency. Nonetheless, nonlinearity dispersion has recently enabled a solution to a long-standing challenge in optics. To explore the potential of this research avenue on solid theoretical grounds, we derive a propagation equation accounting for multifrequency nonlinearities rigorously that maintains the computational advantages of conventional models.

https://doi.org/10.1364/OL.528926

Introduction. Group-velocity dispersion (GVD) together with nonlinear processes sustains important phenomena such as modulation instability, pulse self-compression, solitons, optical wave-breaking, or dispersive wave (DW) emission [1], which have allowed light sources with shorter pulse durations [2], new wavelengths [3], and larger bandwidths [4]. However, the only use of a linear GVD could nowadays be hindering further progress of key enabling components such as fully integrated supercontinuum (SC) sources [5]. Indeed, coherent spectral broadening of ps pulses, namely, one of the challenges preventing that goal, could be achieved exploiting the dispersion of the Kerr nonlinearity [6].

Over the last years, several numerical works have reported how dispersive nonlinearities could dramatically alter modulation instability [6,7], Raman-induced soliton self-frequency shift, or DW emission [8,9]. Moreover, exhibiting an extreme frequency dependence in fibers doped with silver nanoparticles [10], nonlinearities could even reach negative values there, allowing solitons in the normal GVD regime [11–13] and novel bound states of pulses [14]. Earlier, the consequences of mode dispersion on nonlinearities had already been studied theoretically [15–20]. Importantly, these seminal contributions showed that dealing with mode dispersion accurately led to much larger computational demands [16,17]. A formal solution to this problem was developed in Ref. [18] based on a mode expansion in Taylor series around the carrier frequency ω_0. Nevertheless, the number of nonlinear terms grew rapidly with the order of the mode polynomial. This fact tended to restrict its use to cases where the series could be truncated to its lowest orders [19]. A revision of the origin of the problem and how it is currently addressed is now outlined. Our discussion focuses on interactions due to the third-order susceptibility $\chi^{(3)}(-\omega;\omega_1,-\omega_2,\omega_3)$ [21], but similar considerations apply to other nonlinear processes.

As $\chi^{(3)}$ depends on four frequencies, so does the nonlinear coefficient γ. Note that γ also incorporates the mode dispersion at four frequencies [21]. When this multifrequency dispersion is considered, the nonlinear term in the propagation equation is not efficiently calculated by means of Fourier transforms [16,17], contrary to the case where such dependences are neglected [22]. To our knowledge, two approximations have been proposed so far to tackle this issue. First, the generalized nonlinear Schrödinger equation (GNLSE) assumes $\gamma(-\omega;\omega,-\omega,\omega)$ [21]. This approach may suit interactions between neighboring frequencies [17], but the pulse energy and the number of photons are not in general conserved [23,24]. Second, the dependences on the four frequencies are factorized [15,17,20,24]. Although this last method does conserve the pulse energy and the number of photons, it does not admit further improvements.

In this Letter, we show analytically how the nonlinear coefficient depends on multiple frequencies mainly through the mean frequency of each nonlinear interaction. We also demonstrate that the resulting theory conserves the pulse energy and the number of photons, and its nonlinear term can be evaluated using Fourier transforms. As such, this model amends the GNLSE properly and predicts new effects due to the multifrequency nature of the nonlinear-coefficient dispersion (NCD).

Multifrequency nonlinear coefficient. Considering that the nonlinear-coefficient dependence on multiple frequencies is the central problem of this work, lossless waveguides and (real) transverse fields are assumed for the sake of simplicity. The starting point to obtain the multifrequency nonlinear coefficient is the propagation equation for a single-mode electric field $\tilde{\mathbf{E}}(\mathbf{x}_t,z,\omega) = \tilde{G}(z,\omega)\,\mathbf{e}(\mathbf{x}_t,\omega)\,e^{i\beta(\omega)z}$:

$$\frac{\partial \tilde{G}(z,\omega)}{\partial z} = \frac{i}{2}\frac{\omega}{N(\omega)}e^{-i\beta(\omega)z}\int \mathrm{d}^2\mathbf{x}_t\,\mathbf{e}(\mathbf{x}_t,\omega)\cdot\tilde{\mathbf{P}}_{\mathrm{NL}}(\mathbf{x}_t,z,\omega), \quad (1)$$

where $N = \int \mathrm{d}^2\mathbf{x}_t\left[\mathbf{e}(\mathbf{x}_t,\omega)\times\mathbf{h}(\mathbf{x}_t,\omega)\right]\cdot\hat{\mathbf{z}}$ is a normalization factor, $\mathbf{e}$ and $\mathbf{h}$ stand for the electric and magnetic mode fields with propagation constant β, the subindex t denotes transverse components, and $\mathbf{P}_{\mathrm{NL}}$ represents the nonlinear polarization

[15–18,22]. In our case,

$$\tilde{P}_{NL,i} = \frac{\varepsilon_0}{(2\pi)^2}\frac{3}{8}\int \mathrm{d}\omega_1\mathrm{d}\omega_2\mathrm{d}\omega_3\, \chi^{(3)}_{ijkl}(-\omega;\omega_1,-\omega_2,\omega_3)\times \tilde{\mathcal{E}}_j(\omega_1)\tilde{\mathcal{E}}^*_k(\omega_2)\tilde{\mathcal{E}}_l(\omega_3)\,\delta(\omega-\omega_1+\omega_2-\omega_3), \quad (2)$$

where $\tilde{\mathcal{E}}_i$ is the i-component of the analytic signal of the electric field in the frequency domain defined as $\tilde{\mathcal{E}}_i(\omega<0) = 0$, $\tilde{\mathcal{E}}_i(0) = \tilde{E}_i(0)$ and $\tilde{\mathcal{E}}_i(\omega>0) = 2\tilde{E}_i(\omega>0)$ [25] and the dependences on spatial coordinates are omitted. The complex envelope of the pulse in the frequency domain, $\tilde{A}$, is defined via $\tilde{\mathcal{E}}_i(\mathbf{x}_t, z, \omega) = \sqrt{2/N(\omega)}\tilde{A}(z, \omega-\omega_0)\, e_i(\mathbf{x}_t, \omega)\, e^{i\beta_0 z}\, e^{i\beta_1(\omega-\omega_0)z}$, with $\beta_k = \mathrm{d}^k\beta/\mathrm{d}^k\omega|_{\omega_0}$ [17,26]. However, changing to the variable $\tilde{\Psi} = (N(\omega_0)/N(\omega))^{1/2}\tilde{A}$ is convenient here to subsume the factorizable frequency dependences due to normalization factors. Plugging Eq. (2) into Eq. (1) and restricting the resulting equation to positive frequencies,

$$\frac{\partial\tilde{\Psi}}{\partial z} = i\beta_{\mathrm{p}}(\omega)\tilde{\Psi} + i\frac{\eta(\omega)}{(2\pi)^2}\int \mathrm{d}\omega_1\mathrm{d}\omega_2\mathrm{d}\omega_3\, \Gamma^{(3)}(\omega,\omega_1,\omega_2,\omega_3)\times \tilde{\Psi}(\omega_1-\omega_0)\tilde{\Psi}^*(\omega_2-\omega_0)\tilde{\Psi}(\omega_3-\omega_0)\,\delta(\omega-\omega_1+\omega_2-\omega_3), \quad (3)$$

where $\beta_{\mathrm{p}} = \beta - \beta_0 - \beta_1(\omega-\omega_0)$, $\eta = (\omega/c)\, N(\omega_0)/N(\omega)$ and the multifrequency nonlinear coefficient is given by the following:

$$\Gamma^{(3)} = \frac{3\,\varepsilon_0 c}{4\,N^2(\omega_0)}\int \mathrm{d}^2\mathbf{x}_t\, \chi^{(3)}_{ijkl}\, e_i(\omega)e_j(\omega_1)e_k(\omega_2)e_l(\omega_3). \quad (4)$$

For dispersionless Kerr interactions in isotropic media $\chi^{(3)}_{ijkl} = \chi^{(3)}_{xxxx}(\mathbf{x}_t,\omega_0)(\delta_{ij}\delta_{kl} + \delta_{ik}\delta_{jl} + \delta_{il}\delta_{jk})/3$ [1]. Given that the first and third summands of this tensor contribute equally to Eq. (3),

$$\Gamma^{(3)} = \frac{2}{3}\Gamma(\omega,\omega_1,\omega_2,\omega_3) + \frac{1}{3}\Gamma(\omega,\omega_2,\omega_1,\omega_3), \quad (5)$$

with

$$\Gamma(\omega,\omega_1,\omega_2,\omega_3) = \frac{\int \mathrm{d}^2\mathbf{x}_t\, n^2 n_2\, \mathbf{e}(\omega)\cdot\mathbf{e}(\omega_1)\,\mathbf{e}(\omega_2)\cdot\mathbf{e}(\omega_3)}{n^2_{\mathrm{eff}}(\omega_0)\left(\int \mathrm{d}^2\mathbf{x}_t\, \mathbf{e}(\omega_0)\cdot\mathbf{e}(\omega_0)\right)^2}, \quad (6)$$

where $n = n(\mathbf{x}_t,\omega_0)$ and $n_2 = n_2(\mathbf{x}_t,\omega_0)$ are the refractive and Kerr index distributions [1] and n_{eff} is the mode effective index. Note that if mode dispersion is disregarded, Eq. (3) reduces to the following:

$$\frac{\partial A(z,T)}{\partial z} = i\hat{\beta}_{\mathrm{p}} A + i\hat{\gamma} A^* A^2, \quad (7)$$

where $A = \mathcal{F}^{-1}\tilde{A}$, $\mathcal{F}$ is the Fourier transform with conjugated variables $T = t - \beta_1 z$ and $\Omega = \omega - \omega_0$ [1] and the operators $\hat{\beta}_{\mathrm{p}} = \mathcal{F}^{-1}\beta_{\mathrm{p}}(\omega_0+\Omega)\mathcal{F}$ and $\hat{\gamma} = c^{-1}\mathcal{F}^{-1}(\omega_0+\Omega)\Gamma(\omega_0)\mathcal{F}$, with $\Gamma(\omega_0)$ meaning $\Gamma(\omega_0,\omega_0,\omega_0,\omega_0)$, have been introduced. Notwithstanding, if $\mathbf{e}(\mathbf{x}_t,\omega)$ is considered, the coupling between $\mathbf{x}_t$ and ω makes it challenging to reduce the evaluation of the nonlinear term of Eq. (3) to Fourier transforms and products.

Multifrequency nonlinear Schrödinger equation: derivation and conservation of number of photons and energy. Expanding $\mathbf{e}(\mathbf{x}_t,\omega)$ in the Taylor series at the first order around an adaptive frequency ω_m depending on the integration frequencies in Eq. (3), thus different in general to ω_0, which is a fixed frequency, we derive the following:

$$\mathbf{e}(\omega)\cdot\mathbf{e}(\omega_1)\,\mathbf{e}(\omega_2)\cdot\mathbf{e}(\omega_3) \simeq \left[\mathbf{e}(\omega_m)\cdot\mathbf{e}(\omega_m)\right]^2 + \left[\left.\frac{\partial\mathbf{e}}{\partial\omega}\right|_{\omega_m}\cdot\mathbf{e}(\omega_m)\right]\left[\mathbf{e}(\omega_m)\cdot\mathbf{e}(\omega_m)\right](\omega+\omega_1+\omega_2+\omega_3-4\,\omega_m). \quad (8)$$

In light of this result, if ω_m is selected as the mean frequency of each nonlinear process, and $\omega_m = (\omega+\omega_2+\omega_1+\omega_3)/4 = (\omega\ +\ \omega_2)/2$ by virtue of energy conservation, then

$$\Gamma(\omega,\omega_1,\omega_2,\omega_3) \simeq \Gamma(\omega_m,\omega_m,\omega_m,\omega_m). \quad (9)$$

Using $\omega_m = (\omega+\omega_2)/2$, the notation $\Psi_i = \Psi(\Omega_i)$, $\mathrm{d}^3\Omega = \mathrm{d}\Omega_1\mathrm{d}\Omega_2\mathrm{d}\Omega_3$, and $\Gamma(\Omega)$ indicating $\Gamma(\omega_0+\Omega)$, we demonstrate that Eq. (9) allows calculating the nonlinear term of Eq. (3) as follows:

$$\begin{aligned}
&\frac{1}{(2\pi)^2}\int \mathrm{d}^3\Omega\,\Gamma\left(\frac{\Omega+\Omega_2}{2}\right)\tilde{\Psi}_1\,\tilde{\Psi}^*_2\,\tilde{\Psi}_3\,\delta(\Omega-\Omega_1+\Omega_2-\Omega_3) = \\
&\frac{1}{(2\pi)^3}\int \mathrm{d}^3\Omega\,\Gamma\left(\frac{\Omega+\Omega_2}{2}\right)\tilde{\Psi}_1\,\tilde{\Psi}^*_2\,\tilde{\Psi}_3\int \mathrm{d}\tau\, e^{i(\Omega-\Omega_1+\Omega_2-\Omega_3)\tau} = \\
&\frac{1}{2\pi}\int \mathrm{d}\Omega_2\,\Gamma\left(\frac{\Omega+\Omega_2}{2}\right)\int \mathrm{d}t\,\Psi^*(t)\,e^{i\Omega_2 t}\int \mathrm{d}\tau\,\Psi^2(\tau)e^{i(\Omega+\Omega_2)\tau} = \\
&\mathcal{F}\,\Psi^*\,\mathcal{F}^{-1}\,\Gamma\left(\frac{\tilde{\Omega}}{2}\right)\mathcal{F}\,\Psi^2,
\end{aligned} \quad (10)$$

where $\tilde{\Omega}$ refers to the frequency of the Fourier transforms enclosing Γ. Accordingly, from Eq. (3) and under Eq. (9), we derive the multifrequency nonlinear Schrödinger equation (MFNLSE):

$$\frac{\partial\Psi(z,T)}{\partial z} = i\hat{\beta}_{\mathrm{p}}\,\Psi + i\hat{\eta}\,\Psi^*\,\hat{\Gamma}_{\mathrm{K}}\,\Psi^2, \quad (11)$$

where $\hat{\eta} = \mathcal{F}^{-1}\eta(\omega_0+\Omega)\mathcal{F}$ and $\hat{\Gamma}_{\mathrm{K}} = \mathcal{F}^{-1}\Gamma(\omega_0+\Omega/2)\mathcal{F}$. In Eq. (11), the leading error of each contribution to the summation (multiple integral) that defines the nonlinear term in Eq. (3) is of the second order in the difference between its frequencies and *its corresponding* ω_m, but this accuracy can also be improved by expanding the fields to a higher order in Eq. (8). Such an extension is left for future investigation, but it shows that the scope of our approach goes beyond the case studied in this work.

Despite the remarkable simplification of Eq. (11) compared to Eq. (3), the MFNLSE still conserves the number of photons:

$$\begin{aligned}
&\frac{\mathrm{d}}{\mathrm{d}z}\int \mathrm{d}\Omega\,\frac{|\tilde{A}|^2}{(\omega_0+\Omega)} = \frac{\mathrm{d}}{\mathrm{d}z}\int \mathrm{d}\Omega\,\frac{|\tilde{\Psi}|^2}{c\,\eta} = 2\,\mathrm{Re}\left(\int \mathrm{d}\Omega\,\frac{1}{c\,\eta}\tilde{\Psi}^*\frac{\partial\tilde{\Psi}}{\partial z}\right) \\
&= 2\,\mathrm{Re}\left(\frac{i}{c}\int \mathrm{d}\Omega\,\tilde{\Psi}^*\mathcal{F}\,\Psi^*\hat{\Gamma}_{\mathrm{K}}\,\Psi^2\right) = 2\,\mathrm{Re}\left(\frac{i}{c}\,2\pi\int \mathrm{d}t\,(\Psi^*)^2\,\hat{\Gamma}_{\mathrm{K}}\,\Psi^2\right) \\
&= 2\,\mathrm{Re}\left(\frac{i}{c}\int \mathrm{d}\Omega\,\Gamma\left(\omega_0+\frac{\Omega}{2}\right)\left|\mathcal{F}\,\Psi^2\right|^2\right) = 0,
\end{aligned} \quad (12)$$

and the pulse energy:

$$\begin{aligned}
&\frac{\mathrm{d}}{\mathrm{d}z}\int \mathrm{d}\Omega\,|\tilde{A}|^2 = 2\,\mathrm{Re}\left(\frac{i}{c}\int \mathrm{d}\Omega\,(\omega_0+\Omega)\,\tilde{\Psi}^*\mathcal{F}\,\Psi^*\,\hat{\Gamma}_{\mathrm{K}}\,\Psi^2\right) = \\
&2\mathrm{Re}\left(\frac{2\pi}{c}\int \mathrm{d}t\,\frac{\partial\Psi^*}{\partial t}\Psi^*\,\hat{\Gamma}_{\mathrm{K}}\,\Psi^2\right) = \mathrm{Re}\left(\frac{i}{c}\int \mathrm{d}\Omega\,\Omega\,\Gamma\,\left|\mathcal{F}\,\Psi^2\right|^2\right) = 0,
\end{aligned} \quad (13)$$

where the unitarity of Fourier transforms, $\int \mathrm{d}\Omega\,\tilde{\Theta}^*\mathcal{F}\Phi = 2\pi\int \mathrm{d}t\,(\mathcal{F}^{-1}\tilde{\Theta})^*\Phi$, has been used in both proofs.

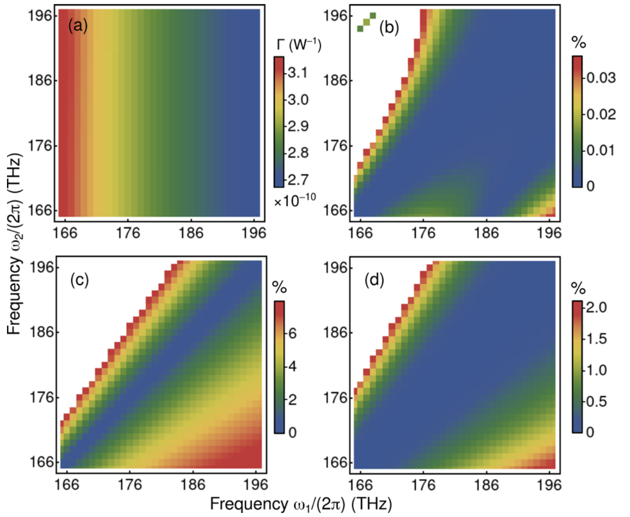

Fig. 1. For degenerate FWM in the LP_{02} mode of the step-index fiber under test, (a) $\Gamma(2\omega_1 - \omega_2, \omega_1, \omega_2, \omega_1)$ and relative errors due to (b) Eq. (9), (c) single-frequency approximation, and (d) factorization (see details in the text). Note the different scales of the color bars.

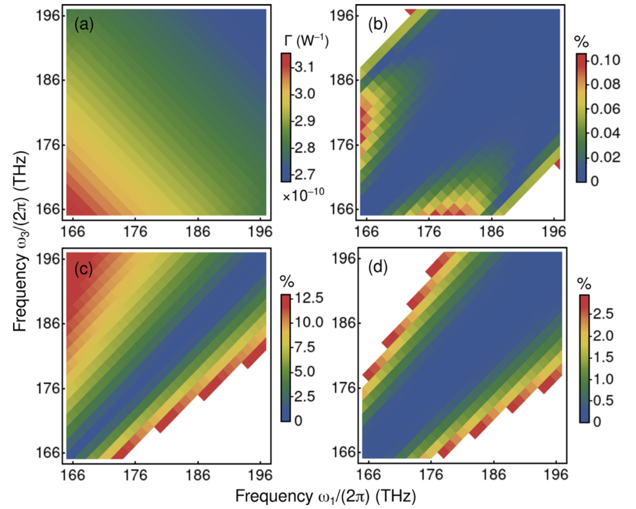

Fig. 2. For nondegenerate FWM in the LP_{02} mode of the step-index fiber under test, (a) $\Gamma(2\omega_3 - \omega_1, \omega_1, 2\omega_1 - \omega_3, \omega_3)$ and relative errors due to (b) Eq. (9), (c) single-frequency approximation, and (d) factorization (see details in the text). Note the different scales of the color bars.

Therefore, the MFNLSE makes it compatible accounting for multifrequency NCD on a solid physical basis with an efficient numerical computation. Even if the Kerr index were responsible for NCD, Eq. (9) could still account for NCD if $\chi^{(3)}_{ijkl}(\omega;\omega_1,-\omega_2,\omega_3) \simeq \chi^{(3)}_{ijkl}(\omega_m;\omega_m,-\omega_m,\omega_m)$. It is worth anticipating that the Raman scattering (RS) will also be incorporated into this theory later.

Comparative analysis of approximations for the multifrequency nonlinear coefficient. To evaluate the accuracy of Eq. (9) undergoing relatively large mode dispersion, a step-index fiber with a 13 µm core diameter and 0.2 numerical aperture is employed. The LP_{02} mode of this fiber experiences the transition from core to cladding confinement at telecom wavelengths, where it also shows anomalous GVD. Note that SC in the LP_{02} mode has been experimentally demonstrated [27]. With this fiber, $\Gamma(\omega,\omega_1,\omega_2,\omega_3)$ are numerically computed for degenerate four-wave mixings (FWM) $2\,\omega_1 \longrightarrow \omega_2 + \left[\omega = \omega_1 - (\omega_2 - \omega_1)\right]$ and nondegenerate FWM $\omega_1 + \omega_3 \longrightarrow \left[\omega_2 = \omega_1 - (\omega_3 - \omega_1)\right] + \left[\omega = \omega_3 + (\omega_3 - \omega_1)\right]$. It is worth mentioning that the output frequencies of these nondegenerate FWM can be stimulated from degenerate FWM where ω_1 or ω_3 acts as the pump. These *exact* values for Γ are compared to our proposal $\Gamma(\omega_m)$, the single-frequency $\Gamma(\omega)$, and the factorization $\left(\Gamma(\omega)\Gamma(\omega_1)\Gamma(\omega_2)\Gamma(\omega_3)\right)^{1/4}$.

Degenerate FWM are studied first. Attending to Fig. 1(a), Γ varies more than 15% over 30 THz. Although the frequency region where the relative error change is more pronounced has not been colored in Fig. (1) in order to visualize meaningful color maps, the next results do account for all frequencies. In Fig. 1(b), the relative error due to Eq. (9) remains below 0.7% with a mean value of 0.024%. The mean and largest errors increase up to 45% and 5600% for the single-frequency approximation in Fig. 1(c) and to 3.2% and 165% for the factorized ansatz in Fig. 1(d).

Nondegenerate FWM are now explored. The rate of change of Γ is similar to the degenerate cases according to Fig. 2(a) and the mean and largest relative errors provided by Eq. (9) are 0.054% and 1.5%, respectively. The counterpart errors for the single-frequency case reach 54% and 6300% in Fig. 2(c) and 7% and 178% when the multifrequency dependence is factorized in Fig. 2(d). Based on this comparative analysis, we conclude that Eq. (9) outperforms the existing alternative modeling multifrequency NCD. In addition, and unlike them, our approach also leaves room for improvement, as explained previously.

Raman scattering in the multifrequency nonlinear Schrödinger equation. The third-order susceptibility of RS in silica is the following:

$$f_R\chi^{(3)}_{xxxx}\left(\tilde{H}_{\mathrm{R},a}(\omega-\omega_1)\delta_{ij}\delta_{kl} + \frac{1}{2}\tilde{H}_{\mathrm{R},b}(\omega-\omega_1)(\delta_{ik}\delta_{jl}+\delta_{il}\delta_{jk})\right), \tag{14}$$

where $H_{\mathrm{R},a(b)}$ denote the Raman response functions [15,28] and f_R represents the Raman fraction [1]. If Eq. (14) is introduced in Eq. (4) and a single nonlinear material is assumed, then

$$\Gamma^{(3)} \simeq f_R\tilde{H}_\mathrm{R}(\omega-\omega_1)\Gamma\left(\frac{\omega+\omega_2}{2}\right), \tag{15}$$

where $\tilde{H}_\mathrm{R} = \tilde{H}_{\mathrm{R},a} + \tilde{H}_{\mathrm{R},b}$ and Eq. (9) has been used. The Raman term resulting from Eq. (15) conserves the number of photons, as can be proven plugging Eq. (15) into Eq. (3) and applying the changes of dummy variables $\omega \leftrightarrow \omega_1$ and $\omega_2 \leftrightarrow \omega_3$, and the hermiticity of $\tilde{H}_R$, $\tilde{H}^*_R(\Omega) = \tilde{H}_R(-\Omega)$, when the number of photons is calculated; see Eq. (12).

Since RS in silica restricts interactions to a frequency range of order $\Omega_\mathrm{R}/(2\pi) \sim 13$ THz [28], $|\Omega - \Omega_2| \sim \Omega_\mathrm{R} \ll \omega_0 + \Omega$ and $\Gamma(\omega_0 + \Omega + (\Omega_2 - \Omega)/2)$ may thus be expanded in the Taylor series around $\omega_0 + \Omega$. Given that Eq. (9) is accurate to the second order, we neglect here second-order contributions to the Taylor series of Γ and consider $\Gamma(\omega+\omega_2)/2) \simeq (\Gamma(\omega)+\Gamma(\omega_2))/2$ to derive the next extension of the MFNLSE accounting for RS:

$$\begin{aligned}\frac{\partial\Psi}{\partial z} &= i\hat{\beta}_\mathrm{p}\,\Psi + i(1-f_R)\hat{\eta}\Psi^*\,\hat{\Gamma}_\mathrm{K}\,\Psi^2 + \\ &\quad i\frac{f_R}{2}\hat{\eta}\left(\hat{\Gamma}\,\Psi\,\hat{H}_\mathrm{R}\,\Psi^*\Psi + \Psi\,\hat{H}_\mathrm{R}\,(\hat{\Gamma}\,\Psi)^*\Psi\right),\end{aligned} \tag{16}$$

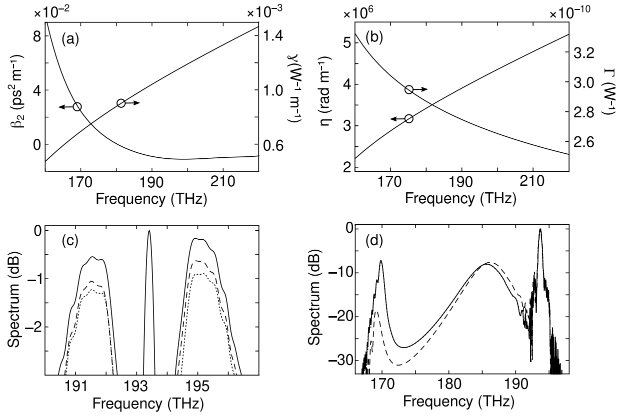

Fig. 3. (a) GVD and GNLSE nonlinearity and (b) MFNLSE nonlinear coefficients. Spectra at 22.2 m without RS (c) and with RS (d) for Eq. (16) (solid lines), GNLSE (dashed lines), and factorization-based equation (dotted lines). Solid and dotted lines are barely distinguishable in (d).

where $\hat{\Gamma} = \mathcal{F}^{-1}\Gamma(\omega_0 + \Omega)\mathcal{F}$ and $\hat{H}_R = \mathcal{F}^{-1}\tilde{H}_R(\Omega)\mathcal{F}$. Note that the Raman term in Eq. (16) is valid beyond the scope of Eq. (9) provided that Γ varies linearly within the Raman bandwidth.

Deviations between nonlinear models. As the equation ruling nonlinear pulse dynamics depends on how Γ is calculated (see Supplement 1), we implement the three nonlinear models derived from the approximations studied in our comparative analysis to explore the propagation of a 0.5-ps-long sech-pulse with 1 kW of peak power at 1.55 µm (~ 193 THz) in the fiber mode handled there. Its GVD and the different NCD profiles are plotted in Figs. 3(a) and 3(b). We first restrict interactions to the Kerr effect. Our model is thus Eq. (16) with $f_R = 0$, i.e., Eq. (11). Under these conditions, the pulse undergoes a periodic higher-order-soliton-like evolution and radiates a DW close to 162 THz [29]. After a few cycles, differences about 1 dB between the output spectra predicted by each theory are observed within a spectral bandwidth of around 5 THz, as Fig. 3(c) illustrates. It is worth noting that, given the accuracy enhancement in Γ that Eq. (11) achieves in view of Figs. 1 and 2, the deviations from Eq. (11) represent discrepancies with respect to Eq. (3).

These simulations are now repeated including RS. The usual Raman response function is employed [1]. In this case, the pulse breaks up after its initial compression and a red-shifting soliton emerges and emits a DW at 170 THz; see Fig. 3(d). Interestingly, this spectral resonance grows much faster when the multifrequency NCD is taken into account, either via Eq. (16) or the factorization-based equation, exceeding by 10 dB its GNLSE counterpart around 22 m. Such a difference vanishes at 30 m, where all theory outcomes become quite similar with a DW relative spectral power about −7 dB (see Supplement 1). This result suggests that the efficiency of DW emission, and hence of SC generation, might increase due to the multifrequency NCD.

In conclusion, a rigorous and practical description of the multifrequency dispersion of nonlinearities has been presented making a convincing case for surpassing traditional models. Moreover, our simulations indicate that the dependence of the nonlinear coefficient on multiple frequencies has observable consequences even in step-index fibers. The theory proposed here could be a key tool to leverage exciting research opportunities enabled by multifrequency nonlinear optics.

Funding. Ministerio de Universidades (María Zambrano Fellowship ZA21-053); European Commission (H2020-MSCA-RISE-2019-872049, María Zambrano Fellowship ZA21-053); Generalitat Valenciana (CIPROM/2022/030).

Disclosures. The authors declare no conflicts of interest.

Data availability. Data underlying the results presented in this Letter are not publicly available at this time but may be obtained from the authors upon reasonable request.

Supplemental document. See Supplement 1 for supporting content.

REFERENCES

1. G. P. Agrawal, *Nonlinear Fiber Optics* (Academic, 2013).
2. Y. Liu, H. Tu, and S. A. Boppart, Opt. Lett. **37**, 2172 (2012).
3. X. Liu, J. Laegsgaard, U. Møller, *et al.*, Opt. Lett. **37**, 2769 (2012).
4. J. M. Dudley, G. Genty, and S. Coen, Rev. Mod. Phys. **78**, 1135 (2006).
5. C.-S. Brès, A. D. Torre, D. Grassani, *et al.*, Nanophotonics **12**, 1199 (2023).
6. D. Castelló-Lurbe, Opt. Lett. **47**, 1299 (2022).
7. N. Linale, J. Bonetti, and D. F. Grosz, Opt. Lett. **45**, 2498 (2020).
8. S. Bose, O. Melchert, S. Willms, *et al.*, Opt. Lett. **46**, 3921 (2021).
9. S. Zhao, R. Guo, and Y. Zeng, Phys. Rev. A **106**, 033516 (2022).
10. A. Lin, X. Liu, P. R. Watekar, *et al.*, Appl. Phys. Lett. **93**, 021901 (2008).
11. S. Bose, A. Sahoo, R. Chattopadhyay, *et al.*, Phys. Rev. A **94**, 043835 (2016).
12. F. R. Arteaga-Sierra, A. Antikainen, and G. P. Agrawal, Phys. Rev. A **98**, 013830 (2018).
13. S. Zhao and X. Sun, Phys. Rev. A **102**, 033514 (2020).
14. O. Melchert, S. Bose, S. Willms, *et al.*, Opt. Lett. **48**, 518 (2023).
15. P. V. Mamyshev and S. V. Chernikov, Opt. Lett. **15**, 1076 (1990).
16. M. Kolesik, E. M. Wright, and J. V. Moloney, Appl. Phys. B **79**, 293 (2004).
17. J. Laegsgaard, Opt. Express **15**, 16110 (2007).
18. T. X. Tran and F. Biancalana, Opt. Express **17**, 17934 (2009).
19. F. Biancalana, T. X. Tran, S. Stark, *et al.*, Phys. Rev. Lett. **105**, 093904 (2010).
20. X. Zhao, A. V. Gorbach, and D. V. Skryabin, J. Opt. Soc. Am. B **30**, 812 (2013).
21. Q. Lin, O. J. Painter, and G. P. Agrawal, Opt. Express **15**, 16604 (2007).
22. P. L. François, J. Opt. Soc. Am. B **8**, 276 (1991).
23. K. J. Blow and D. Wood, IEEE J. Quantum Electron. **25**, 2665 (1989).
24. J. Bonetti, N. Linale, A. D. Sánchez, *et al.*, J. Opt. Soc. Am. B **36**, 3139 (2019).
25. S. Amiranashvili and A. Demircan, Adv. Opt. Technol. **2011**, 989515 (2011).
26. M. Conforti, A. Marini, T. X. Tran, *et al.*, Opt. Express **21**, 31239 (2013).
27. Y. Chen, Z. Chen, W. J. Wadsworth, *et al.*, Opt. Express **21**, 17786 (2013).
28. Q. Lin and G. P. Agrawal, Opt. Lett. **31**, 3086 (2006).
29. D. Castelló-Lurbe, N. Vermeulen, and E. Silvestre, Opt. Express **24**, 26629 (2016).

Supplemental Document

Optics Letters

Multifrequency nonlinear Schrödinger equation: supplement

David Castelló-Lurbe,[1,2,*] **Enrique Silvestre,**[1,3] **and Miguel V. Andrés**[1,2]

[1] *Institut Universitari de Ciències dels Materials, Universitat de València, Catedrático Agustín Escardino 9, Paterna 46980, Spain*
[2] *Departament de Física Aplicada i Electromagnetisme, Universitat de València, Dr. Moliner 50, Burjassot 46100, Spain*
[3] *Departament d'Òptica i Optometria i Ciències de la Visió, Universitat de València, Dr. Moliner 50, Burjassot 46100, Spain*
[*] *david.castello-lurbe@uv.es*

Supplement DOI: https://doi.org/10.6084/m9.figshare.26404423

Parent Article DOI: https://doi.org/10.1364/OL.528926

Multifrequency nonlinear Schrödinger equation: supplemental document

This supplemental document describes the nonlinear models that, together with the multifrequency nonlinear Schrödinger equation, have been employed in Section 6 in the main manuscript. Complementary simulations obtained from these models are also included.

1. FORMER NONLINEAR MODELS

Under the approximations $N(\omega_{1,2,3}) \simeq N(\omega)$ and $\Gamma(\omega,\omega_1,\omega_2,\omega_3) \simeq \Gamma(\omega)$, Eq. (3) in the main manuscript becomes the generalized nonlinear Schrödinger equation (GNLSE) [1],

$$\frac{\partial A(z,T)}{\partial z} = i\hat{\beta}_p A + i(1-f_R)\hat{\gamma}\, A^* A^2 + i f_R \hat{\gamma}\, A\, \hat{H}_R A^* A, \tag{S1}$$

where $\hat{\gamma} = \mathcal{F}^{-1}\gamma(\omega)\mathcal{F}$ with

$$\gamma(\omega) = \frac{\displaystyle\int \mathrm{d}^2\mathbf{x}_t\, n^2 n_2 \left(\mathbf{e}(\omega)\cdot\mathbf{e}(\omega)\right)^2}{n_{\text{eff}}^2(\omega)\left(\displaystyle\int \mathrm{d}^2\mathbf{x}_t\, \mathbf{e}(\omega)\cdot\mathbf{e}(\omega)\right)^2}. \tag{S2}$$

Alternatively, if $\Gamma(\omega,\omega_1,\omega_2,\omega_3) \simeq (\Gamma(\omega)\Gamma(\omega_1)\Gamma(\omega_2)\Gamma(\omega_3))^{1/4}$ is assumed, and the complex envelope $\Theta = \mathcal{F}^{-1}(\Gamma(\omega)/\Gamma(\omega_0))^{1/4}\mathcal{F}\Psi = \mathcal{F}^{-1}(\Gamma(\omega)/\Gamma(\omega_0))^{1/4}(N(\omega_0)/N(\omega))^{1/2}\mathcal{F}A$ is defined, Eq. (3) in the main manuscript leads to the propagation equation

$$\frac{\partial \Theta(z,T)}{\partial z} = i\hat{\beta}_p \Theta + i(1-f_R)\hat{\gamma}_F\, \Theta^* \Theta^2 + i f_R \hat{\gamma}_F\, \Theta\, \hat{H}_R \Theta^* \Theta, \tag{S3}$$

where $\hat{\gamma}_F = \mathcal{F}^{-1}\eta(\omega)(\Gamma(\omega)\Gamma(\omega_0))^{1/2}\mathcal{F}$ [2]. Attending to Ref. [3], this factorization could amount to assume a linear mode-profile dispersion, $\mathbf{e}(\omega) = \mathbf{e}(\omega_0) + \partial_\omega \mathbf{e}|_{\omega_0}(\omega-\omega_0)$, where ω_0 is the carrier frequency. It is crucial to note the difference with respect to our expansion of the electric field around an adaptive frequency ω_m that depends on the integration frequencies of Eq. (3) in the main text. It is precisely this local character of ω_m which makes the multifrequency nonlinear Schrödinger equation (MFNLSE) more general than Eq. (S3). On the one hand, should the mode profile depend on frequency nonlinearly, the MFNLSE would still be valid provided frequencies belonging to different ranges of locally linear mode dispersion would not interact. On the other hand, should such interactions occur, $\Gamma(\omega,\omega_1,\omega_2,\omega_3)$ could also be calculated to a higher order of accuracy and the MFNLSE extended correspondingly along the lines of its current derivation in the main text, while keeping its original computational advantages.

2. NUMERICAL TESTS OF THE PHOTON-NUMBER CONSERVATION

In Fig. S1(a), we plot the evolution of the relative change of the number of photons under Eq. (16) in the main manuscript, Eq. (S1) and Eq. (S3). On the one hand, the variation of the number of photons along the propagation distance below 0.02% indicates that the approximation made in Eq. (16) to describe Raman scattering is very accurate. On the other hand, the law of photon number conservation is violated by 10% over 30 m due to Eq. (S1), while only by 0.3% when Eq. (S3) is used in the simulations. These results are in line with the fact that Eq. (S1) does not necessarily conserve the number of photons while Eq. (S3) does [2]. Finally, Fig. S1(b) shows how the spectra predicted by Eq. (16), Eq. (S1) and Eq. (S3) agree well with each other at 30 m.

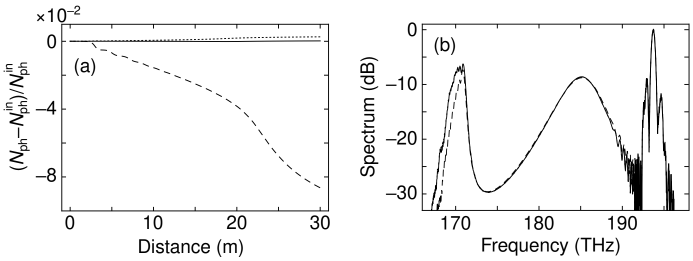

Fig. S1. (a) Relative change of the number of photons N_{ph} and (b) spectra at 30 m predicted by Eq. (16) in the main text (solid line), Eq. (S3) (dotted line, in (b) indistinguishable from the solid line), and Eq. (S1) (dashed line).

REFERENCES

1. G. P. Agrawal, *Nonlinear Fiber Optics* (Academic, 2013).
2. X. Zhao, A. V. Gorbach, and D. V. Skryabin, "Dispersion of nonlinearity in subwavelength waveguides: derivation of pulse propagation equation and frequency conversion effects," J. Opt. Soc. Am. B **27**, 812–820 (2013).
3. J. Lægsgaard, "Mode profile dispersion in the generalized nonlinear Schrödinger equation," Opt. Express **15**, 16110–16123 (2007).